Chapter 3

The Weak Electrolyte Model

I know that I know nearly nothing, and hardly this.

K. R. Popper

Many features of EHC in the conductive range of low frequencies are quantitatively described by the SM, in particular the threshold voltage as function of the external frequency, and the existence and angle of oblique rolls. Nevertheless, even qualitative features remain unexplained. Most notable are travelling rolls which have been observed as early as 1978 [38]. Later on, they were found in a broad parameter range in different liquid crystals (MBBA, Phase 5 and I52) by different groups [42, 39, 40, 41, 30], and seem to be generic for relatively thin and clean cells. Despite this, they have withstood a theoretical understanding until recently.

3.1 Physical assumptions

A theory of travelling rolls in EHC must explain the following facts.

- The travelling rolls are really produced by a Hopf bifurcation that breaks spontaneously the reflection symmetry. This is shown by spatiotemporal correlations of subcritical director fluctuations which are left-right symmetric [39]. This is confirmed by experiments where the control parameter (rms voltage) is modulated in time and, for a modulation with the double Hopf frequency, parametric resonance leads to standing waves as predicted by theory for a Hopf bifurcation [40]. This means that the travelling rolls really originate from a Hopf bifurcation to degenerate right and left travelling rolls. Drift effects due to broken left-right symmetry (e.g., nonideal planar boundary conditions with a pretilt [52, 76]) are excluded.

- Travelling rolls are only found in thin cells, e.g., in MBBA in cells with $d = 13\mu m$ [39], but not in cells with $d \geq 20\mu m$ [41, 43], and in I52 for $d = 28\mu m$, but not for $d = 57\mu m$ [30, 42].

- For a fixed cell thickness, travelling rolls are observed for conductivities below a certain threshold [30]. From experiments, it was suggested [31], that deviations from the SM scale with $(\sigma_\perp d^2)^{-1}$ and, in particular, that for a given material the codimension-two curve separating stationary from travelling rolls is given by $\sigma_\perp d^2 = $ const.

- For a stongly negative dielectric anisotropy (MBBA with $\epsilon_a = -0.53$ or Phase 5 with ϵ_a of the order of -0.2) one observes travelling rolls only in a certain frequency range $\omega_{0,min} < \omega_0 < \omega_{cutoff}$ (e.g. between 350 and 420 Hz in [40]), or, the Hopf frequency becomes very low for low frequencies [41, 78]. For I52 at low temperatures (slightly negative ϵ_a) there are travelling rolls with a significantly nonzero Hopf frequency for all frequencies and the Hopf frequency increases with the external frequency. At high temperatures (ϵ_a essentially zero) the Hopf curve of I52 is essentially flat [30, 42].

- Furthermore, there is an excellent quantitative agreement between the SM and experiments for *thermal* convection in NLCs [23, 79, 24], so any new model must reduce to the SM for zero electric fields, and for large values of $\sigma_\perp$ and d^2.

In the SM, the static and dynamic electric properties of the NLC are described by $\boldsymbol{D} = \underline{\epsilon}\boldsymbol{E}$ and $\boldsymbol{J} = \underline{\sigma}\boldsymbol{E}$, respectively. Obviously, a new model must generalize either of these two relations.

The static relation has been generalized to include flexoelectric effects (see Chapter 2.2), $\boldsymbol{D} = \underline{\epsilon}\boldsymbol{E} + P_{flexo}$ [49, 65]. The *rationale* was that the flexoelectric terms break the combined symmetry $z \rightarrow -z$, $t \rightarrow t + \pi/\omega_0$ and that the resulting coupling of two linear modes, namely the conductive IA and dielectric IIB modes (see Chapter 5.2) may lead to oscillations at threshold [52]. However, this can be the case only for external frequencies where both modes get unstable nearly simultaneously (crossover), i.e. only near the cutoff frequency. In addition, there are other problems with the flexoeffect that are described in Chapter 2.2. Anyway, evaluating the SM including the flexoeffect has not led to travelling rolls.

A generalization of $\boldsymbol{J} = \underline{\sigma}\boldsymbol{E}$, i.e., a non-ohmic conductivity, was suggested already in the Refs. [48, 52] and will be the basis of the development of the WEM. The intrinsic conductivity of thermotropic NLCs is extremely low (for I52 less than $10^{-9}(\Omega m)^{-1}$

[31]; To obtain a sufficient and well-controlled conductivity, one adds often an ionizable dopant to the NLC. For MBBA with the dopant *Tetrabutyl-Ammonium Tetraphenyl-Boride* (TBATPB), the conductivity increases with the square root of the TBATPB concentration [80]; with a molar concentration of 10^{-5} moles per liter one obtains a conductivity of $1.5 \times 10^{-7} (\Omega m)^{-1}$. For I52, it proved to be very difficult to find a dopant providing enough conductivity for EHC, probably because I52 consists of nonpolar molecules, in contrast to MBBA. At last (after 17 tries with other dopants) a concentration of 2% (!) Iodine (I_2) was successful in the experiments of Mike Dennin [31].

For MBBA with the dopant TBATPB, the measured dependence of the equilibrium conductivity from the square root of the TBATPB concentration can be naturally explained by a simple dissociation-recombination reaction. Ref [80] suggests the reaction

$$(C_4H_9)_4\ N(C_6H_5)_4B \rightleftharpoons (C_4H_9)_4\ N^+ + (C_6H_4)_4B^-,$$
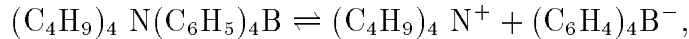
which has the generic form [80]

$$AB \rightleftharpoons A^+ + B^-.$$
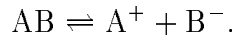
In equilibrium, the product of the number densities n^+ and n^- of the ions A^+ and B^- is proportional to the density n_{AB} of the undissociated molecules, $n^+n^-/n_{AB} = $ const. $:= K$ (mass-action law). The conductivity is caused by the drift of the dissociated ions, is proportional to the sum of n^+, n^-, weighted with the mobilities. With typical values for the mobilities (see Table 3.1) one finds that only a small fraction of the impurities is dissociated into ionic charge carriers (weak-electrolyte limit) and one obtains from the mass-action law the observed square-root behaviour. In the I_2 doped I 52, the molecules form a charge-transfer complex and then undergo a dissociation-recombination reaction [31]. Although this is a multistep process, the net effect should be described by the above simple binary reaction.

In any case, the current should be described as in the SM (Ohm's law with anisotropic conductivities) for homogeneous stationary systems, or, approximatively, for thick cells. This motivates following assumptions for the WEM.

- The electric current is caused by two species of ionic charge carriers A^+ and B^- with charges $\pm e$ [1] and number densities n^+ and n^-. The electric current $\boldsymbol{J}^\pm$ of each species is caused by advection with the fluid velocity, migration

---

[1]Charges of $\pm ne$ can be taken care of by renormalizing the mobility by a factor of $1/n$.

(drift) by electric fields $\boldsymbol{E}$, and diffusion due to carrier-density gradients [81],

$$
\begin{aligned}
\boldsymbol{J} = \boldsymbol{J}^+ + \boldsymbol{J}^- &= e(n^+ - n^-)\boldsymbol{v} + e\left(\underline{\underline{\mu}}^+ n^+ + \underline{\underline{\mu}}^- n^-\right)\boldsymbol{E} \\
&- e\left(\underline{\underline{D}}^+ \boldsymbol{\nabla} n^+ - \underline{\underline{D}}^- \boldsymbol{\nabla} n^-\right).
\end{aligned} \tag{3.1}
$$

- The charge carriers originate from dissociation of impurity ions and can be described by the net reaction AB $\rightleftharpoons$ A$^+$ + B$^-$ with the dissociation rate $\dot{n}_{diss} = k_d n_{AB}$ and the recombination rate $\dot{n}_{\text{rec}} = k_r n^+ n^-$. In addition, overall neutrality, $\int d^3 r (n^+ - n^-) = 0$, is assumed.

- The mobilities (and diffusivities) are uniaxial tensors whose principal values $\mu_\perp^\pm$ and $\mu_\parallel^\pm$ ($D_\perp^\pm$ and $D_\parallel^\pm$) do not depend on $\boldsymbol{E}$, n^+ or n^-. I assume equal relative anisotropies [80, 28], which must be given by the measured relative anisotropy of the conductivities to be consistent with the SM limit,

$$
\mu_{ij}^+ = \mu_\perp^+ \mu_{ij}', \quad \mu_{ij}^- = \mu_\perp^- \mu_{ij}' \quad \text{with} \quad \mu_{ij}' = \delta_{ij} + \frac{\sigma_a^{eq}}{\sigma_\perp^{eq}} n_i n_j. \tag{3.2}
$$

- The number density of dissociated ions is much lower than the density of the remaining undissociated impurities (weak-electrolyte limit),

$$
n_{AB} >> n^+, n^-. \tag{3.3}
$$

Introducing the dissociation constant $K = k_d/k_r$, the equilibrium charge carrier density of the neutral NLC, $n_0 := n_{eq}^+ = n_{eq}^- = \sqrt{n_{AB}^{eq} K}$, the total concentration of the dopant, $c = n_{AB} + (n^+ + n^-)/2$ (a conserved quantity), and the degree of ionization in equilibrium, $\beta_c = n_0/c$ [28], we have in equilibrium ($E_0 = 0$), but not restricted to weak electrolytes

$$
\beta_c = \frac{K}{2c}\left(\sqrt{1 + 4\frac{c}{K}} - 1\right). \tag{3.4}
$$

The weak-electrolyte limit is given by $\beta_c \approx \sqrt{K/c} << 1$, i.e. $K << c$ which is well satisfied for I52, see Table 3.1. The generalized condition (3.3) for $\boldsymbol{E} \neq 0$ requires knowledge of the solutions of the WEM equations, i.e. can be verified only *a posteriori*.

3.2 Formulation of the WEM

3.2.1 Dynamical equations for the charge- carrier densities

The hydrodynamic part of the equations for the carrier densities (without dissocia-
tion and recombination) can be formulated in the framework of generalized hydro-
dynamics. The electric part $\tilde{\phi}d\rho$ of the SM energy density (2.10) becomes

$$d\epsilon_{el} = \tilde{\phi}e(dn^+ - dn^-) + k_B T d(n^+ \ln n^+ + n^- \ln n^-), \qquad (3.5)$$

where the second term equals T times the additional entropy from the two (non-
interacting) carrier densities. Without dissociation and recombination, the fields $n^{\pm}$
are true hydrodynamic variables obeying the continuity eqations $\partial_t n^{\pm} + \boldsymbol{\nabla} \cdot (n^{\pm}\boldsymbol{v} + \boldsymbol{J}_{n\pm}) = 0$, where the currents are linear combinations of the thermodynamic forces,

$$\boldsymbol{F}^{\pm} = -\boldsymbol{\nabla}\left(\frac{\partial \epsilon}{\partial n^{\pm}}\right) = \pm e\boldsymbol{E} - k_B T \boldsymbol{\nabla} \ln n^{\pm}. \qquad (3.6)$$

Cross couplings between, e.g., $\boldsymbol{J}_{n+}$ and $\boldsymbol{F}^-$ are not forbidden, but it seems reasonable
to neglect them, putting $\boldsymbol{J}_{n\pm} = \underline{\underline{M}}^{\pm}\boldsymbol{F}^{\pm}$. The Onsager matrices $\underline{\underline{M}}^{\pm}$ are determined
by the condition that the ohmic SM conductivity should be recovered in the homo-
geneous limit and by the assumption of constant mobilities ($\boldsymbol{J}_{n\pm} \propto n^{\pm}$). This leads
to $\underline{\underline{M}}^{\pm} = \frac{1}{e}\underline{\underline{\mu}}^{\pm}n^{\pm}$ or

$$\boldsymbol{J}_{n\pm} = \pm\underline{\underline{\mu}}^{\pm}\left(n^{\pm}\boldsymbol{E} - \frac{k_B T}{e}\boldsymbol{\nabla}n^{\pm}\right) \qquad (3.7)$$

Comparison of (3.7) with (3.1) gives a relation of the diffusivities with the mobilities,
the anisotropic form of the Einstein law [28],

$$\underline{\underline{D}}^{\pm} = V_T\underline{\underline{\mu}}^{\pm}, \quad V_T = \frac{k_B T}{e} \approx 26\text{mV}, \qquad (3.8)$$

where V_T is the thermal voltage. The (non-hydrodynamic) dissociation and recom-
bination parts are given in a homogeneous (stirred) system by the usual kinetic
equations $\partial_t n^{\pm} = k_d n_{AB} - k_r n^+ n^-$. The weak-electrolyte assumption implies that
$n_{AB} \approx n_{AB}^{eq} = \text{const}$, or $k_d n_{AB} - k_r n^+ n^- \approx k_r(n_0^2 - n^+ n^-)$.

Combining the hydrodynamic and the non-hydrodynamic parts and substituting
Eq. (3.7) for the currents give the dynamical equations for the carrier densities,

$$\partial_t n^{\pm} + \boldsymbol{\nabla} \cdot \left[\boldsymbol{v}n^{\pm} + \mu_{\perp}^{\pm}\underline{\underline{\mu}}'(\pm\boldsymbol{E} - V_T\boldsymbol{\nabla})n^{\pm}\right] = k_r(n_0^2 - n^+ n^-). \qquad (3.9)$$

Note that, using $\boldsymbol{\nabla}\cdot\boldsymbol{v} = 0$, the left-hand side of (3.9) can be written in the "advective"
form

$(\partial_t + \boldsymbol{v}^\pm \cdot \boldsymbol{\nabla})n^\pm + \mu_\perp^\pm \left(\pm n^\pm \boldsymbol{\nabla}(\underline{\underline{\mu}}'\boldsymbol{E}) - V_T(\boldsymbol{\nabla}n^\pm)(\boldsymbol{\nabla}\underline{\underline{\mu}}') \right)$ where $\boldsymbol{v}^\pm = \boldsymbol{v} + \mu_\perp^\pm \underline{\underline{\mu}}'(\pm\boldsymbol{E} - V_T\boldsymbol{\nabla})$ are the total velocities of the carriers.

In view of coupling Eqs.(3.9) to the director and momentum-balance equations of the SM, it is convenient to write the equation as a continuity equation for the charge density $\rho(\boldsymbol{r},t) = e(n^+ - n^-)$ and a balance equation for the local conductivity $\sigma_\perp(\boldsymbol{r},t) = e(\mu_\perp^+ n^+ + \mu_\perp^- n^-)$,

$$\partial_t \rho \;\; + \;\; \boldsymbol{\nabla} \cdot \left[\rho\boldsymbol{v} + \underline{\underline{\mu}}'\boldsymbol{E}\sigma_\perp - V_T\underline{\underline{\mu}}'\boldsymbol{\nabla}\left(d_1\sigma_\perp + 2\mu s_1\rho\right) \right] = 0, \tag{3.10}$$

$$\partial_t \sigma_\perp \;\; + \;\; \boldsymbol{\nabla} \cdot \left[\sigma_\perp\boldsymbol{v} + \mu\underline{\underline{\mu}}'\boldsymbol{E}(d_1\sigma_\perp + \mu s_1\rho) - \mu V_T\underline{\underline{\mu}}'\boldsymbol{\nabla}\left(s_2\sigma_\perp + d_1\mu s_1\rho\right) \right]$$

$$= \;\; k_r n_0 \sigma_\perp^{eq} \left[1 - \frac{(\sigma_\perp + \mu_\perp^- \rho)(\sigma_\perp - \mu_\perp^+ \rho)}{(\sigma_\perp^{eq})^2} \right], \tag{3.11}$$

where we introduced the effective mobility $\mu = \mu_\perp^+ + \mu_\perp^-$, the equilibrium conductivity $\sigma_\perp^{eq} = \mu e n_0$ and the mobility ratio $\gamma = \mu_\perp^-/\mu_\perp^+$ together with $d_1 = (1 - \gamma)/(1 + \gamma)$, $s_1 = \gamma/(1 + \gamma)^2$, and $s_2 = (1 + \gamma^2)/(1 + \gamma)^2$. Note that the terms $\propto s_1, s_2 (\propto d_1)$ are (anti-) symmetric with respect to a change $n^+ \leftrightarrow n^-$ corresponding to $\gamma \to 1/\gamma$. $\sqrt{s_1}$ is the ratio of the geometric mean to the sum of the mobilities.

3.2.2 Boundary conditions

In the structureless state with no variations in x and y, we have $\rho = \epsilon_\perp \partial_z E_z$, and Eqs. (3.10) and (3.11) represent, with respect to the z derivatives, a third-order equation for E_z and a second-order equation for $\sigma_\perp$. Thus we need at the confining plates five BCs for the electrical variables in addition to the usual fully-rigid planar SM-BCs $\boldsymbol{n} = (1, 0, 0)$ and $\boldsymbol{v} = 0$ ($z = \pm d/2$). The integral condition

$$\int_{-d/2}^{d/2} dz \; E_z = V(t) \tag{3.12}$$

is always valid. the remaining four electrical BC are relations between current, electric field and density for each species at the electrodes which can depend in a complicated way on electrochemical processes and may be parametrised e.g., for $z = d/2$ as

$$J_z^\pm = \sigma_{\text{surface}}^\pm E_z - D_{surface}^\pm(n_{ext}^\pm - n^\pm), \tag{3.13}$$

where $\boldsymbol{J}^+ = e\boldsymbol{J}_n^+$ ($\boldsymbol{J}^- = -e\boldsymbol{J}_n^-$) are the electric currents carried by the positive (negative) carriers. Some special cases are

- Strongly injecting electrodes where σ_{surface} is very large at one or at both electrodes leading to $E_z = 0$ ("space-charge limiting conditions"). In the isotropic-unipolar case, such BCs are adopted, e.g., in the Refs. [81, 82].

- Electrodes absorbing outflowing carriers, $\sigma_{\text{surface}}^{\pm} = e\mu_{\perp}^{\pm}n^{\pm}$ for $\boldsymbol{E} \cdot \hat{e} > 0$, and $\sigma_{\text{surface}} = 0$ for $\boldsymbol{E} \cdot \hat{e} < 0$ ($\hat{e}$ is the outwards-pointing normal vector). This kind of electrodes is used for electrodyalitic purification [83].

- The BCs of the SM. For zero diffusivities, the five electric BC lead to an overdetermined system. This fixes the BC to the "ohmic BC" $\sigma_{\text{surface}}^{\pm} = e\mu_{\perp}^{\pm}n^{\pm}$ or $J_z = \sigma_{\perp}E_z$.

- Blocking electrodes. No transfer of any charge through the electrodes [84, 85, 86],

$$J_z^+(z = \pm d/2) = J_z^-(z = \pm d/2) = 0. \tag{3.14}$$

These last BCs do not involve unknown electrochemical processes and will be assumed in the rest of this paper. They are also relevant for the I52 experiments (insulating SI O_2 - layer at the electrodes [30]) and it is known that, for AC driving, blocking electrodes do not influence EHC [87]. These BC imply that the total charge $\int_{cell} d^3r\rho := \int dx\, dyQ$ is a conserved quantity. Usually, overall neutrality ($Q = 0$) is assumed, but the electrodes may contain as well permanently adsorbed charges [86]. This can be incorporated into the WEM by setting

$$E_z(d/2) - E_z(-d/2) = -\frac{Q_{ad}}{\epsilon_0\epsilon_{\perp}}, \tag{3.15}$$

where Q_{ad} is the average adsorbed total charge per area and E_z is the field just inside the layers. Remarkably, Eq. (3.15) is the same whether the charges are adsorbed at the top or bottom plates or on both, see Fig. 3.1. Like the flexoeffect, adsorbed charges break the z symmetry of the system, but leave the combined symmetry $z \to -z$, $t \to t + \pi/\omega_0$ intact. Adsorbed charge layers increase the Fre'edericksz threshold in a simple model [86]. Their effect on EHC has not been investigated.

3.2.3 Material parameters related to conductivity

In addition to the SM material parameters (see e.g. Ref. [48] for MBBA), the Eqs. (3.10) and (3.11) contain the WEM parameters $\mu_{\perp}^+, \mu_{\perp}^-$, and $k_r n_0$. As will be shown later, only the products $\mu_{\perp}^+\mu_{\perp}^-$ and $k_r n_0$ are relevant, in most cases.

Table 3.1: Material parameters related to conduction

parameter	material	value and source
total mobility μ ##	MBBA [++] MBBA 5CB theory for MBBA	3.71 [80]; 0.18 [83]; 1..10 [87]; 10 [81]; 1 [28] 0.6 [84]; 2.5 [86] 11 (Stokes friction) [80] 0.2 (dielectric friction) [87]
geometric mean $\sqrt{\mu_\perp^+ \mu_\perp^-}$	I52	0.40 ... 0.47 (Hopf frequency) [42]
assumed mobility ratio γ	MBBA[#] 5CB	1 [80] $\gg 1$ [84]
mobility anisotropy $\frac{\mu_a}{\mu_\perp}$	MBBA	0.33 [80]; 0.5 [88]
dissociation constant $K = \frac{k_d}{k_r}$	MBBA[#] MBBA [††]	$3.4 \times 10^{21} \mathrm{m}^{-3}$ [80] $(2..4) \times 10^{20} \mathrm{m}^{-3}$ [28]
recombination-rate constant k_r	MBBA [†] dielectric liquids	$1.5 \times 10^{-27} \mathrm{m}^3 \mathrm{s}^{-1}$ [83] $10^{-15} \mathrm{m}^3 \mathrm{s}^{-1}$ [81]
carrier lifetime $\tau_{\mathrm{rec}} = (2 k_r n_0)^{-1}$	MBBA [†] MBBA 5CB	2.7×10^4 s [83] 10^{-3} s [81] 0.05 s [86]
equilibrium density n_0	MBBA 5CB	$6 \times 10^{20} \mathrm{m}^{-3}$ [28] $10^{20} \mathrm{m}^{-3}$ [84]; $8 \times 10^{20} \mathrm{m}^{-3}$ [85]
degree of ionization $\beta_c = \frac{n_0}{c}$, Eq. (3.4)	MBBA [*, #] I52 [,+]	0.001 0.2
diffusion constant D	5CB	$4.5 \times 10^{-13} \mathrm{m}^2 \mathrm{s}^{-1}$ [84]

In units of $10^{-10} \mathrm{m}^2/(\mathrm{Vs})$;   # dopant TBATPB;
†† dopants TBAP and TBAB;   ++ does not depend on the TBATPB concentration;
† electrodialysed to $\sigma = 5 \times 10^{-9} (\Omega \mathrm{m})^{-1}$, 50 °C(3K above the clearing point);
** dopant 2% I$_2$;   * For $\sigma_\perp = 10^{-7} (\Omega \mathrm{m})^{-1}$, $\mu_\perp = 3.71 \times 10^{-10} \mathrm{m}^2/(\mathrm{Vs})$;
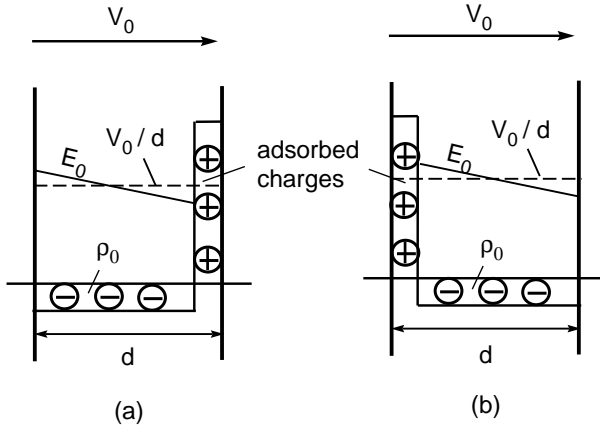+ T=40C, $\sigma_\perp = 0.49 \times 10^{-8} (\Omega \mathrm{m})^{-1}$

Figure 3.1   Effects of adsorbed surface charges on the electric field and the volume charges under the assumption of an otherwise trivial basic state (discussed in Chapter 4. (a): Charges adsorbed at the right (top) plate; (b): Charges adsorbed at the left (bottom) plate. For illustrative purposes, the δ-distributed surface charge is drawn as a layer of finite thickness.

The dissociation constant K and the total mobility $\mu = \mu_\perp^+ + \mu_\perp^-$ (and thus n_0) were measured in MBBA doped with TBATPB [80] by fitting the experimentally obtained conductivity *vs.* concentration curve to the expression obtained from (3.4),

$$\sigma_\perp^{eq}(c) = e\mu n_0 = e\mu\beta_c c = \frac{e\mu K}{2}\left(\sqrt{1 + 4\frac{c}{K}} - 1\right). \tag{3.16}$$

The quantities μ, $k_D n_{AB} \approx k_d c$ and k_r were determined by measuring the stationary current and the current response to various voltage signals in electrodialytic cells with charge-absorbing BC [83]. Another group used the current response in cells with blocking BC to measure μ, n_0 and indirectly the diffusion constant D via the thickness of the diffusive boundary layers [84, 85, 86] which are assumed to decay exponentially with the Debye length λ_D, see Table 3.2. The resulting diffusivity is smaller by a factor of three than that obtained with the Einstein relation. As discussed in Chapter 4, the thickness of the diffusive boundary layers can be obtained also by measuring the capacitance as a function of the external frequency [31].

There exist also theoretical estimates for the mobility. In the simplest case one assumes that the dissipation leading to a finite mobility is caused by Stokes's friction of a sphere with the effective ion radius (of the order of 5 Å). For NLCs, the resulting mobilities are two to three orders of magnitude too high [80]. The correct order of magnitude is obtained [87] by assuming additional dissipation from the lag of the polarization cloud in the surrounding solvent [89]. This theory of "dielectric friction", however, predicts an isotropic mobility depending on microscopic parameters like the ion radius and the Debye relaxation time ($\approx 10^{-6}$ s in NLCs [29]) which causes the lag, It is applicable only to polar solvents (MBBA, not I52). Finally, the WEM relates the geometric mean $\sqrt{\mu_\perp^+\mu_\perp^-}$ to the Hopf frequency, see Chapter 5.

Table 3.1 contains a summary of relevant measurements. There seem to be no

Table 3.2: Intrinsic scales of the WEM

quantity	definition	typical value[*]
threshold voltage	$V_{c0} = \sqrt{\frac{K_{11}\pi^2}{\epsilon_0\epsilon_\perp}}$	2.63 V
thermal voltage	$V_T = \frac{k_B T}{e}$	26 mV
diffusion time	$\tau_{\text{diff}} = \frac{d^2}{D^{phys}} \approx \frac{V_{c0}}{V_T}\tau_t$	342 s
recombination time	$\tau_{\text{rec}} = (2k_r n_0)^{-1}$	$10^{-3}...2\times 10^4$ s
carrier transition time	$\tau_t = \frac{d^2}{\mu V_{c0}}$	3.39 s
director relaxation time	$\tau_d = \frac{\gamma_1 d^2}{K_{11}\pi^2}$	0.561 s
charge relaxation time	$\tau_q = \frac{\epsilon_0\epsilon_\perp}{\sigma_\perp}$	5.35×10^{-3} s
momentum diffusion time	$\tau_{\text{visc}} = \frac{d^2 \rho_m}{\gamma_1}$	6×10^{-6} s
diffusion layer	$\lambda_D = \sqrt{\frac{V_T \epsilon_0\epsilon_\perp}{2en_0}} = \sqrt{\frac{V_T \epsilon_0\epsilon_\perp \mu}{2\sigma_\perp^{eq}}}$	0.1 μm
[*] NLC I52 for $d = 28$ μm at $T = 40°$C (see Appendix A.1)		

measurements of γ although this seems to be possible by the current-response experiments.

3.2.4   Intrinsic times and lengths, scaling

In the Table 3.2 I show the various intrinsic time, length and voltage scales of the WEM subsystems. One sees that the full WEM has the potential for rich behaviour. Note that, by virtue of the Einstein law, the diffusion scales are not connected with new material parameters. It is useful to scale lengths, times, the electric potential and the total charge concentration in such a way that they become of the order of unity for EHC. The chosen scaling is given in Table 3.3. Many properties of the SM do not depend on the absolute values of the material parameters (in contrast to the WEM), so the material constants will be scaled as well. Dependent quantities are scaled accordingly, e.g., $\boldsymbol{E}$ in units of $V_{c0}\pi/d$ and ρ in units of $V_{c0}\pi^2\epsilon_0\epsilon_\perp/d^2$. Furthermore, it is sometimes useful to express the local conductivity in terms of the deviation from its equilibrium value,

$$\delta\sigma(\boldsymbol{r}, t) := \frac{\sigma_\perp(\boldsymbol{r}, t)}{\sigma_\perp^{eq}} - 1. \tag{3.17}$$

Table 3.3: Scaling

quantity	scaling unit	typical value [*]
lengths	d/π	$(10...100\mu\text{m})/\pi$
time	$\tau_d = \frac{\gamma_1 d^2}{K_{11}\pi^2}$	0.166 s $\left(\frac{d}{10\mu m}\right)^2$
voltage	$V_{c0} = \sqrt{\frac{\pi^2 K_{11}}{\sigma_\perp \tau_q}} = \sqrt{\frac{\pi^2 K_{11}}{\epsilon_0 \epsilon_\perp}}$	1.19 V
conductivities	$\sigma_\perp^{\text{eq}} = \mu e n_0$	$10^{-9}...10^{-7}(\Omega\text{m})^{-1}$
orientational elasticities	K_{11}	$6.66 \times 10^{-12}\text{N}$
dielectric constants	$\epsilon_0 \epsilon_\perp$	$4.65 \times 10^{-11}\text{As/Vm}$
viscosities	$\gamma_1 = \alpha_3 - \alpha_2$	0.109 kg (m s)$^{-1}$
[*] parameter set MBBA I (Appendix A.1)		

Unless explicitely stated otherwise, all variables with the exception of the scaling units $\epsilon_\perp, \sigma_\perp^{\text{eq}}, \gamma_1$, and K_{11} are understood as scaled variables in the rest of this thesis.

The resulting scaled WEM equations, which replace the SM equations (2.24)-(2.26), are an important building block of this work and the basis for the investigations in the next three chapters. They read

$$P_1(\partial_t + \boldsymbol{v} \cdot \boldsymbol{\nabla})\rho = -\boldsymbol{\nabla} \cdot (\underline{\mu'}\boldsymbol{E}\sigma) + \tilde{D}\boldsymbol{\nabla}\underline{\mu'}\boldsymbol{\nabla}\left(\rho + \frac{\tilde{d}\sigma}{2P_1\pi^2\tilde{\alpha}^2}\right) \quad (3.18)$$

$$(\partial_t + \boldsymbol{v} \cdot \boldsymbol{\nabla})(\sigma - \tilde{d}\rho) = -\tilde{\alpha}^2\pi^2\boldsymbol{\nabla} \cdot (\underline{\mu'}\boldsymbol{E}\rho) + \frac{\tilde{D}}{P_1}\boldsymbol{\nabla}\underline{\mu'}\boldsymbol{\nabla}\left(\sigma - \frac{\tilde{d}\rho}{2}\right) \quad (3.19)$$

$$- \frac{\tilde{r}}{2}\left[(\sigma+1)(\sigma-1) - \tilde{d}\rho\sigma - P_1\pi^2\tilde{\alpha}^2\rho^2\right]$$

$$(\partial_t + \boldsymbol{v} \cdot \boldsymbol{\nabla})\boldsymbol{n} = \boldsymbol{\omega} \times \boldsymbol{n} + \underline{\delta}^\perp\left(\lambda\underline{A}\boldsymbol{n} - \boldsymbol{h}\right) \quad (3.20)$$

$$\frac{\tau_{\text{visc}}}{\tau_d}(\partial_t + \boldsymbol{v} \cdot \boldsymbol{\nabla})v_i = -\partial_i p - \partial_j(T_{ij}^{\text{visc}} + \pi_{ij}) + \pi^2\rho E_i, \quad (3.21)$$

The system parameters R, ω_0, P_1, $\tilde{\alpha}$ and $\tilde{r}$ are given in Table 3.4, $\tilde{d} = (P_1/\gamma)^{1/2}\pi(1-\gamma)\tilde{\alpha}$ is a mobility-difference parameter and $\tilde{D} = 4s_1(\pi\lambda_D/d)^2$ the scaled diffusion constant. [2] The constitutive equations for ρ, $\boldsymbol{h}$ and T_{ij}^{visc} are, respectively, given by $\boldsymbol{\nabla} \cdot (\underline{\epsilon}\boldsymbol{E})$, Eq. (2.27), and Eq. (2.28) with the scaled material

---

[2]In contrast to the SM Eq. (2.24), the diffusion currents have been kept in Eqs. (3.18) and (3.19). The approximation of zero diffusivities is usually assumed in the bulk. This may not be justified for very thin cells where the thicknes of the boundary layers can become of the same order as d (Chapter 4.) Furthermore, in the dielectric regime where the size of the patterns can be $<< d$. the neglect of the diffusivities becomes questionable even in the bulk.

parameters and ϵ_a replaced by $\pi^2 \epsilon_a$ in Eq. (2.27). The electric field

$$\boldsymbol{E} = \sqrt{2R}\cos\omega_0 t \,\hat{z} - \boldsymbol{\nabla}\phi \tag{3.22}$$

contains the two SM-control parameters. The fully rigid BC for homogeneous alignment and blocking electrodes are

$$\int_{-\pi/2}^{\pi/2} dz \ E_z = \sqrt{2R}\cos\omega_0 t, \tag{3.23}$$

$$[J_z]_{z=\pm\pi/2} = \left[E_z\sigma - \tilde{D}\partial_z\left(\rho + \frac{\tilde{d}\sigma}{2P_1\pi^2\tilde{\alpha}^2}\right)\right]_{z=\pm\pi/2} = 0, \tag{3.24}$$

$$[J_z^\sigma]_{z=\pm\pi/2} = \left[-\tilde{\alpha}^2\pi^2 E_z\rho + \frac{\tilde{D}}{P_1}\partial_z(\sigma - \tilde{d}\rho/2)\right]_{z=\pm\pi/2} = 0, \tag{3.25}$$

$$\boldsymbol{n}(\pm\pi/2) = (1,0,0), \quad \boldsymbol{v}(\pm\pi/2) = 0. \tag{3.26}$$

3.3   Discussion

The physical contents of the new Eq. (3.19) is an excitation of the charge-carrier mode (σ mode) by the ρ mode $\propto \tilde{\alpha}^2$, diffusion $\propto \tilde{D} \propto \tilde{\alpha}^2$ and recombination $\propto \tilde{r}$. [3]

The WEM equations (3.18) - (3.26) contain much more parameters as other fluid-dynamical systems. For example, the scaled Boussinesq equations for RBC in simple fluids depend only on the Rayleigh number and the Prandtl number $\tau_{\mathrm{therm}}/\tau_{\mathrm{visc}}$. The WEM contains two "Rayleigh-number like" control parameters R and ω_0, four "Prandtl-number like" time-scale ratios of subsystems, P_1, $\tilde{\alpha}$, $\tilde{r}$ and $\tau_{\mathrm{visc}}/\tau_d$, one ratio of WEM material parameters, γ, and a total of eight ratios of SM material parameters, $K_{22}, K_{33}, \epsilon_\perp, \sigma_\perp$ and four viscosities.

Fortunately, the dynamics is mainly determined by the first two classes ("system parameters"), summarized in Table 3.4. The ratio $\tau_{\mathrm{visc}}/\tau_d$ can always be neglected (at least in the conductive range), i.e. the velocities can be adiabatically eliminated. In many cases, also the charge can be adiabatically eliminated, $P_1 = 0$.

The full WEM equations (3.18) to (3.21) seem too complex for direct theoretical investigations. Fortunately, the typical parameters given in the tables in the last section suggest some simplifications, depending on the particular situation. In the following, I discuss the approximations of zero diffusivity, of a linear recombination term and of zero mobility difference parameter $\tilde{d}$, which are used for the linear

---

[3]For a nonzero mobility difference, these effects act on a linear combination of the carrier and the charge-density fields, but it will be shown that the parts $\propto \tilde{d}$ can be neglected in most cases.

Table 3.4: System parameters of the WEM

parameter	physical process	MBBA[#]	I52[##]
$R = \frac{\overline{V}^2}{V_{c0}^2} = \frac{\overline{V}^2 \epsilon_0 \epsilon_\perp}{K_{11}\pi^2}$	control parameter	≥ 31	≥ 14
$\omega_0 P_1 = \omega_0^{phys} \tau_q = \frac{\omega_0 \epsilon_0 \epsilon_\perp}{\sigma_\perp}$	control parameter	$0 \cdots 2.5$	$0 \cdots 4$
$P_1 = \frac{\tau_q}{\tau_d} = \frac{\epsilon_0 \epsilon_\perp K_{11}\pi^2}{\sigma_\perp \gamma_1 d^2}$	charge relaxation	0.0095	0.00356
$\tilde{\alpha} = \frac{\sqrt{s_1 \tau_q \tau_d}\pi}{\tau_t} = \sqrt{\frac{\mu_\perp^+ \mu_\perp^- \gamma_1 \pi^2}{\sigma_\perp^{eq} d^2}}$	ion migration	0.0253	0.024
$\tilde{r} = \frac{\tau_d}{\tau_{\mathrm{rec}}} = 2k_r n_0 \tau_d$	recombination	0.05*	0.05*

[#] Parameter set MBBA I with $d = 13\mu$m,
$\quad \sigma_\perp = 10^{-8}(\Omega\mathrm{m})^{-1}, \mu = 10^{-10} m^2/(Vs), \gamma = 1$.
[##] Parameters from Appendix A.1 for 40C; especially
$\quad d = 28\mu$m, $\sigma_\perp^{eq} = 0.493 \times 10^{-8}(\Omega\mathrm{m})^{-1}$, $\mu = 0.88 \times 10^{-10} m^2/(Vs)$, $\gamma = 1$.
* Estimates, see Chapter 5.5

and nonlinear calculations in Chapters 4 - 6. The approximations are valid in the conductive regime, for not too extemely different mobilities and for $\tilde{\alpha} << 1$, i.e. for not too thin cells and not too high mobilities. In addition, I discuss the limits where the SM is recovered and relate various models used in the literature to special cases of the WEM.

3.3.1 Approximations for low mobilities in the conductive range

The thickness of the boundary layers, as deduced from the capacitance measurements [31], is about 1 μm. This is of the same order as the thickness of the boundary layer estimated from the WEM (see Chapter 4). The value of the diffusivity given directly in Table 3.1 as well as that obtained indirectly from the mobilities by the Einstein relation (3.8) lead to Debye lengths even well below 1 μm (Table 3.4). So it seems reasonable, to neglect the diffusive boundary layers, at least in the conductive range and for not too thin cells. There are some subtleties connected with the BC. The equations (3.23) to (3.25) lead to an overdetermined system and impose the BC $E_z = 0$ or $\rho = 0$ and $\sigma = 0$. This is, of course, plausible since the drift current cannot be balanced by a diffusive current to satisfy the blocking BC, so its z component must be zero. This is fulfilled either for $E_z = 0$ or, if there are no carriers at all. On the other hand, a vanishing diffusivity *and* a vanishing mobility (leaving $\sigma_\perp$

constant) means boundary layers of vanishing thickness representing a capacitor of infinite capacity. For the carriers, this is an infinite sink and leads, as in the SM, to "free" electric BC $\partial_z E_z = \partial_z \sigma = 0$, no matter what the real BCs are.

There is one *caveat* connected with ion drift. For zero dissociation and recombination, a DC voltage together with blocking BC would lead to a complete charge separation (the bulk is free of carriers) after the time $\tau_t/\sqrt{R}$. For a nonzero dissociation with $\tau_{\rm rec}/\tau_t << 1$, the total density of the (dissociated and non-dissociated) impurities will decay on a (larger) time scale $\tau_t/(\sqrt{R}\beta_c)$ (electrodialysis). [4] With an AC voltage these separation effects occur only near the electrodes, within the distance over which a carrier can migrate in one half-cycle, see Eq. (4.6) below. For most experiments (especially for those on I52) this distance is comparable to that of the thickness of the diffusion layer and both boundary effects can be neglected.

If $\tilde{\alpha} << 1$ (which is fulfilled unless the mobilities are extremely high or the cell is extremely thin), the recombination term can be treated in linear order, even for nonlinear calculations. For EHC in the conductive regime, the typical amplitude of the carrier mode normalized to the charge-density mode is $||\sigma||/||\rho|| = \mathcal{O}(\pi\tilde{\alpha}^2\sqrt{R_c}/\tilde{r})$ or $\mathcal{O}(\pi\tilde{\alpha}^2\sqrt{R_c}/\omega_H) = \mathcal{O}(\pi\tilde{\alpha}/\sqrt{R_c})$, whichever is lower ($\omega_H$ is related to the Hopf frequency, Chapter 5 below and $||*||$ here denotes the amplitude). This means that even in the fully nonlinear regime where $||\rho|| = \mathcal{O}(1)$ all recombination terms in the bracket of (3.19) are of the order of $\tilde{\alpha}^2 << 1$.

The only mobility-difference term surviving the above approximations is that on the left-hand side of (3.19). If $\tilde{r}$ is sufficiently low, so that the condition for a Hopf bifurcation is fulfilled (Chapter 5), the relative magnitude $\tilde{d}||\rho||/||\delta\sigma|| = \mathcal{O}(P_1 R_c/\gamma)^{1/2}/(1-\gamma)/\pi)$ is usually small. In addition, the $\tilde{d}$ term has the z and time symmetry opposite to that of as the σ mode and does not couple back to the WEM mechanism. With all these approximations the WEM equations (3.18) - (3.20) become

$$P_1(\partial_t + \boldsymbol{v} \cdot \boldsymbol{\nabla})\rho \;=\; -\boldsymbol{\nabla} \cdot (\underline{\mu'} \boldsymbol{E}\sigma) \tag{3.27}$$

$$(\partial_t + \boldsymbol{v} \cdot \boldsymbol{\nabla})\sigma \;=\; -\tilde{\alpha}^2\pi^2\boldsymbol{\nabla} \cdot (\underline{\mu'} \boldsymbol{E}\rho) - \tilde{r}\delta\sigma, \tag{3.28}$$

$$(\partial_t + \boldsymbol{v} \cdot \boldsymbol{\nabla})\boldsymbol{n} \;=\; \boldsymbol{\omega} \times \boldsymbol{n} + \underline{\delta}^{\perp}\left(\lambda\underline{\underline{A}}\boldsymbol{n} - \boldsymbol{h}\right), \tag{3.29}$$

$$\rho|_{z=\pm\pi/2} \;=\; \partial_z\sigma|_{z=\pm\pi/2} = 0. \tag{3.30}$$

---

[4]In this and further order-of-magnitude estimates of drift distances, I assume, for simplicity, the upper bound μ for the mobility of the faster drifting charge-carrier species.

3.3.2 The limit of the Standard Model

Equation (3.27) reduces to the charge conservation of the SM for $\sigma = 1$ or $\delta\sigma = 0$. Since the magnitude of $\delta\sigma$ scales with $\tilde{\alpha}^2/\tilde{r}$, this is the case for $\tilde{\alpha} \to 0$ while $\tilde{r} \neq 0$. In Chapter (3.3.1) it is argued that the boundaries behave effectively as the ohmic BC of the SM if the boundary layers have a thickness $<< d$. With the results from Chapter 4 this is fulfilled for $\tilde{\alpha} << 1$, $\tilde{\alpha}/\tilde{r} << 1$ and $\tilde{\alpha}\sqrt{P_1}/(\omega_0^{phys}\tau_q) << 1$ (ω_0^{phys} is the external frequency in unscaled physical units).

All above conditions for the SM limit can be summarized as

$$\tilde{\alpha} \to 0, \quad \tilde{r} \neq 0, \quad \omega_0 \neq 0. \tag{3.31}$$

3.3.3 Relation with models assuming fast recombination

In the limit of fast dissociation and recombination, the carrier mode can be adiabatically eliminated by setting the bracket of Eq. (3.19) equal to zero. Inserting the resulting $\sigma(\rho)$ into (3.18) (where in contrast to (3.27) the diffusivity is retained) leads to a "bipolar charge conservation" equation for ρ, which is different from the SM for $\tilde{\alpha} \neq 0$. Coupling this equation to an isotropic momentum balance equation (Eq. (3.21) with $\alpha_4 \to 2\eta$ and all other viscosities set equal to zero) gives for a DC voltage the model investigated by Turnbull [81]. Linear analysis for injecting (rather than blocking) BC gives a convective DC instability [81], which, of course, takes place also in isotropic fluids containing carriers.

In the unipolar limit $\rho \to \infty$, $n^+ >> n^-$ ($\rho \to -\infty$, $n^+ << n^-$) corresponding to strongly injecting electrodes, this model reduces to that considered by Felici and contains also a DC instability [90, 82].

At last, the fast-recombination limit of the WEM is obtained by coupling the bipolar charge conservation $\sigma(\rho)$ to the Eqs. (3.20) and (3.21) and assuming an AC voltage and blocking BC. This model leads to an increase for the threshold of EHC, but again, no Hopf bifurcation [91]. The threshold shift is plausible since, in contrast to the injecting BC for the DC instabilities [82, 90], the change of the volume force in the direction of the force is positive, $\rho E_z \partial_z (\rho E_z) > 0$ i.e. the volume forces of the basic state act in the stabilizing direction.